ELSEVIER

Organic Electronics

materials • physics • chemistry • applications

Editors

Chihaya Adachi
Paul Heremans
René Janssen
Antoine Kahn

(This is a sample cover image for this issue. The actual cover is not yet available at this time.)

Ambient laser direct-write printing of a patterned organo-metallic electroluminescent device

Nicholas T. Kattamis [a], Neil D. McDaniel [b], Stefan Bernhard [b], Craig B. Arnold [a,*]

[a] Princeton University, Mechanical and Aerospace Engineering, Engineering Quad Room D214, Princeton, NJ 08544, USA
[b] Carnegie Mellon University, Department of Chemistry, 4400 Fifth Avenue, Pittsburgh, PA 15213, USA

ARTICLE INFO

ABSTRACT

In this work we use laser direct-write (LDW) to fabricate patterned $[Ru(dtb\text{-}bpy)_3]^{2+}(PF_6^-)_2$ electroluminescent devices under ambient processing conditions. Device fabrication is accomplished via laser micromachining of a transparent conducting oxide top electrode, LDW printing the active organo-metallic material, and vapor depositing the bottom electrode. Nuclear magnetic resonance spectroscopy is used to ensure the transfer of damage-free luminophore material. Devices tested in air are shown to exhibit emission spectra, luminous efficiencies, and lifetimes similar to literature values for devices fabricated in nitrogen environments. The versatility of laser direct-write printing is then demonstrated by printing multi-color luminophore patterns with diameters down to 10 μm for future use in high-resolution device fabrication. This approach is compatible with large-area organic electronics that require the fabrication of high-resolution architectures.

© 2011 Elsevier B.V. All rights reserved.

1. Introduction

Advances in organic electronic materials have created an attractive alternative to traditional semiconductor devices. Organic materials have the advantage of being compatible with large area, lightweight and flexible plastic substrates and can be inexpensive to fabricate [1–4]. A particular subset of these materials, namely ionic transition metal complexes (iTMCs), has drawn much attention due to the high mobility of charge carrying ions in the organic layer. These materials enable single-layer device architectures that are more economical to manufacture and electronically more versatile than typical organic devices allowing the use of alternating currents [5]. Higher mobilities mitigate electrode work function limitations, permitting the use of oxygen-stable metal electrodes [6]. Lastly, the use of small molecule iTMCs alleviate problems with purification often encountered in polymer-based devices [7].

Device fabrication typically consists of spin coating solutions of iTMCs over transparent conducting electrodes. However, this approach is limited in its ability to produce high-resolution features without additional processing. Such features are important when fabricating multicolor displays and other more advanced light-emitting and electronic device architectures. Instead, direct-write printing techniques have the advantage of depositing organic material directly into high-resolution patterns without masks, molds, or the need for subsequent patterning steps [8,9].

Laser-induced forward transfer (LIFT) has emerged as a versatile technique for producing direct-write patterns of organic electronic materials [10–13] or direct printing of intact multilayer OLED structures [14–16]. In its conventional form [8], the bottom of a laser-transparent glass substrate (donor) is coated with an ink and placed 50–500 μm above a receiver substrate. Upon pulsed-laser irradiation, a confined region of ink near the glass interface is vaporized, and ink volumes as small as picoliters [17] are ejected onto the receiver substrate. User-programmable pattern generation is enabled through three-dimensional, sub-micron motion control of the donor/receiver assembly relative to the laser source. The direct-write nature of LIFT eliminates

* Corresponding author.
  E-mail address: cbarnold@princeton.edu (C.B. Arnold).

the need for masks used in vapor deposition and is often chosen over nozzle based methods when higher viscosity inks are required or the unreliable characteristic of nozzle clogging must be avoided. In addition, the entire LIFT process is conducted in ambient conditions making it a cost effective and convenient technique for the rapid prototyping of novel devices.

When dealing with organic molecules, LIFT presents a number of challenges. For instance, special care must be taken when the material of interest is particularly susceptible to thermal, optical, or mechanical damage [11]. Conversely, when the ink material does not strongly absorb incident laser energy, transmitted radiation inevitably interacts with the receiver substrate and can cause undesired vaporization of the transparent conducting oxide. The addition of foreign materials in the ink to absorb the laser can enable transfer in these cases but can also quench electroluminescence and hinder device operation.

To avoid these drawbacks we incorporate a polymer film absorbing layer (thickness = 2–8 μm) between the glass substrate and ink material on the donor [11,18,19]. Upon laser irradiation, a small volume of polymer nearest the polymer/glass interface absorbs the energy, forming an enclosed high pressure vapor that deforms the remaining polymer film into the adjacent ink and induces its transfer. This modified LIFT technique is termed blister-actuated laser-induced forward transfer (BA-LIFT) because the ink transfer is a consequence of laser-generated blister motion (Fig. 1a). BA-LIFT eliminates possible contamination issues associated with laser-absorbing additives or thinner laser absorbing layers by tuning the process for the absorption of laser energy solely in the polymer film and by selecting a thick enough polymer layer that will not fully decompose. In addition, BA-LIFT has been shown to successfully deposit weak laser-absorbing organic and biological materials, including systems that are optically and thermally sensitive [11,19].

In this work we use ambient laser direct-write techniques for fabricating patterned $[Ru(dtb-bpy)_3]^{2+}(PF_6^-)_2$ (Complex 1) electroluminescent devices. To confirm the viability of the BA-LIFT process for printing damage-free luminophore molecules, nuclear magnetic resonance (NMR) spectroscopy is employed. Our devices are characterized by acquiring emission spectra and measuring luminous efficiencies and lifetimes, which are similar to literature values of devices fabricated in nitrogen environments. Finally we demonstrate the versatility of BA-LIFT, by printing multi-color luminophore patterns for future use in high-resolution device fabrication.

2. Experimental

The two employed iTMC examples are tris(4,4′-di-tert-butyl-2,2′-bipyridyl)ruthenium, $[Ru(dtb-bpy)_3](PF_6)$ [20] (Complex 1), and bis(5-trifluoromethyl,2-(2′,4′-difluoro-phenyl)pyridyl), (4,4′-di-tert-butyl-2,2′-bipyridyl)iridium, $[Ir(F_5-mppy)_2(dtb-bpy)](PF_6)$ [21] (Complex 2), both of which are prepared as previously described [20,21]. In the absence of a blue-emitting iTMC, 9-anthracenemethanol (Aldrich, 97%, Complex 3) is selected as a surrogate, and used without further purification.

Donor substrates are produced by soaking glass slides in a solution of NOCHROMIX and sulfuric acid to remove oils and loosen debris. Slides are subsequently washed in deionized water, rinsed with acetone and ethanol, and blow dried with nitrogen. Slides are then spin coated with commercially available polyimide (HD Microsystems PI2525) at different spin speeds (3000 and 6000 RPM), and cured as in previous work to produce final film thicknesses of approximately 7 μm and 4 μm, respectively [19]. Luminophore solution is subsequently spread onto donor substrates with a wirecoater, or an aliquot of solution is drop cast onto donor substrates and spun at 1000 rpm
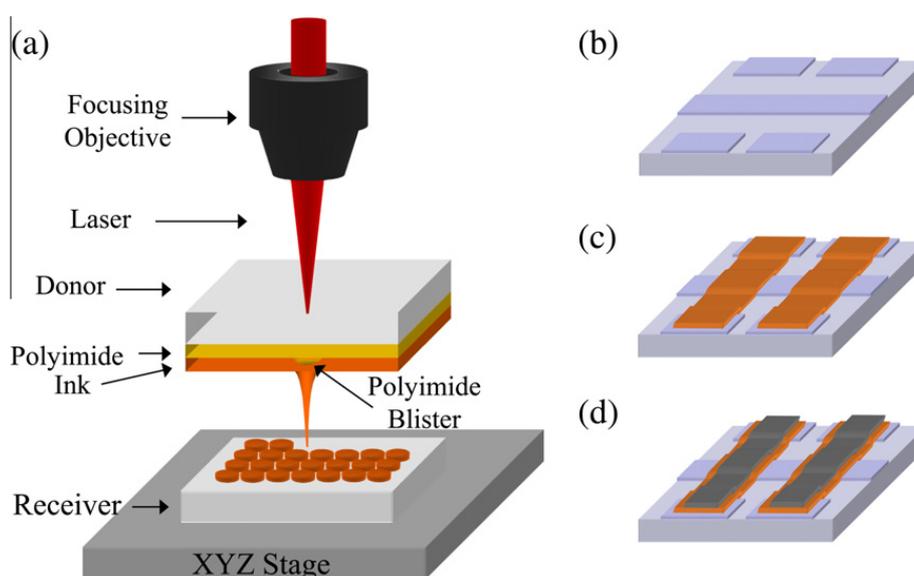

Fig. 1. (a) Illustration of the BA-LIFT process depicting ink transfer in the form of a coherent jet. Device fabrication begins with (b) laser micromachined indium tin oxide coated glass followed by (c) BA-LIFT printing of the organic ink in ambient conditions defining two 3.5 × 12.5 mm² pads. (d) Vapor deposition of the aluminum bottom electrode completes the fabrication process.

for 20 s. Wirecoating produces a donor film thickness of 10 μm and is used to print luminophore material for the device and for the NMR measurements. Spin coating decreases the donor film thickness (1 μm) and is used to print multi-color luminophore patterns. For NMR spectroscopy and multi-color patterning experiments, solutions are created for each complex by adding 38 mg of the complex into a solution of acetonitrile/N-methyl-2-pyrrolidone (NMP, 1/1 v/v, 1 mL). This is heated to 50 °C for 5 min to dissolve the solute. For electroluminescent device fabrication Complex **1** (38 mg) is added to the same solvent (1 mL) with an addition of poly(methyl methacrylate) (PMMA, 6 mg).

Device fabrication begins by laser micromachining the electrically isolated Indium Tin Oxide (ITO) patterns in Fig. 1b. This is accomplished with a Nd:YVO$_4$ laser (λ = 355 nm, τ = 20 ns) at a laser fluence of 0.5 J/cm^2. Polyimide donor substrates and ITO receiver substrates are cleaned in acetonitrile prior to the deposition of the organo-metallic layer. Complex **1** luminophore solution is subsequently wirecoated onto a donor substrate and held at a 100 μm distance from the ITO receiver. Transfer is with the same laser focused to a 10 μm diameter at the glass/polyimide interface (fluence = 2.5 J/cm^2). The BA-LIFT process produces arrays of overlapping voxels that form two uniform pads as shown in Fig. 1c. The receiver is then dried in vacuum for 1 h to evaporate the remaining solvent. The aluminum bottom electrode is vapor deposited through a shadow mask to a final thickness of 50 nm at a rate of 1–2 Å/s. This produces two pixels located at the intersection of the top and bottom electrode (2.5 × 2.5 mm^2 each, Fig. 1d).

Photoluminescence measurements are carried out using an Hg lamp equipped with an optical filter centered at 370 nm. The devices are pre-biased to 4 V for 3 min to assist the drift of PF$_6^-$ counterions to the ITO electrode, followed by a quick ramp to a higher voltage (~6 V) to ensure the device turns on. All emission spectra are recorded with a colorimeter and are later normalized by peak intensity. Time-dependent electroluminescent measurements are conducted from pristine devices without a pre-bias. For NMR measurements ½ mL of deuterated acetone is used to rinse the luminophore material off the ITO acceptor slides. For droplet characterization printed arrays are illuminated and images are captured with a fluorescent microscope equipped with a standard CCD camera.

3. Results and discussion

An image of the working device is shown in Fig. 2a. Under room light illumination, two bands of printed luminophore (orange–red hue) are visibly wider than the aluminum electrode, eliminating the possibility of shorting between the top and bottom electrodes. Under forward bias (ITO+, Al−), bright electroluminescence is visible from the pixels (Fig. 2b). The uniformity of the electroluminescence suggests that the ITO electrode remains undamaged during the BA-LIFT process, since damage would impede uniform charge transfer across the electrode and into the active material.

Charge injection in this organo-metallic molecule differs from typical small molecule organics due to the presence of mobile counterions. In forward bias, PF$_6^-$ counterions migrate towards the ITO electrode [5], creating high electric fields in its vicinity, aiding the injection of holes to the highest occupied molecular orbital of the [Ru(dtb-bpy)$_3$]$^{2+}$ metal center [6,7]. This depletes the region near the aluminum electrode of PF$_6^-$ ions, enhancing the injection of electrons to the lowest unoccupied molecular orbit of the [Ru(dtb-bpy)$_3$]$^{2+}$ ligand. This implies that for a given voltage, device current and light emission are time dependent quantities that depend on the extent of counterion migration. To mitigate this behavior, turn-on time can either be reduced by the addition of an ionic solvent containing PF$_6^-$ counterions [5,21] or through pre-biasing the device [22], the later of which is done in this work according to the prior literature [5,23].

We characterize the emission spectrum of the printed Complex **1** film via photoluminescence (PL) as shown in Fig. 2c. The PL spectrum of the printed luminophore matches the non-printed control solution, with a peak wavelength (630 nm) analogous to literature values [20,22,24]. This ensures that the photoluminescent properties of the molecule are not altered during the BA-LIFT process. Similarly, a direct match in peak wavelength (630 nm) and shape is present between the electroluminescence (EL) and PL spectra in Fig. 2c, indicating undamaged electroluminescent properties. Similar results are available for devices fabricated in nitrogen environments from a spin coated solution of Complex **1** [20,22]. This implies that the presence of air and moisture during the fabrication and testing of our device does not alter its
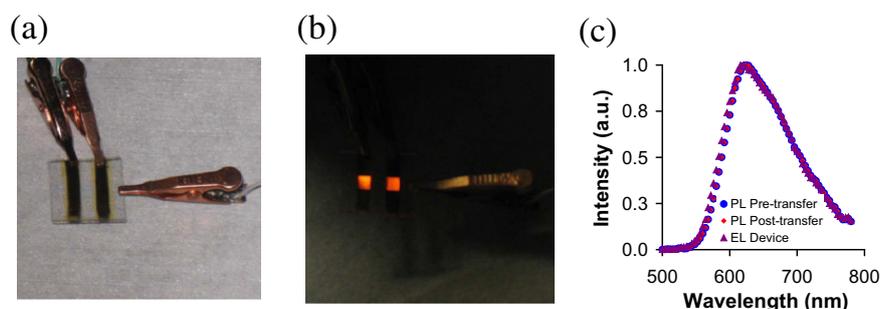

Fig. 2. (a) Image of the device (12.5 × 12.5 mm^2) under room light illumination. (b) Device operation under ambient conditions depicting two 2.5 × 2.5 mm^2 orange–red pixels. (c) Post-transfer PL and device EL match the pre-transfer solution PL. (For interpretation of the references to colour in this figure legend, the reader is referred to the web version of this article.)

emission spectrum and verifies the air tolerance of this complex.

Molecular damage, which can limit device performance, cannot always be properly detected via PL and EL spectroscopy. To ensure the printing of non-damage molecules, NMR spectra are acquired using a procedure described in our earlier work [11]. Fig. 3 depicts the NMR results for the green and red molecules featured in this manuscript. The NMR spectra for the blue molecule are given in earlier work [11] and reproduced here for comparison. Spectra of samples printed via BA-LIFT are depicted in (d–f), and corresponding control samples are in (a–c). As seen, samples printed via BA-LIFT produce identical NMR spectra to control samples, indicating the absence of molecular damage during the printing process. This ensures that device performance, as in the case of the $[Ru(dtb-bpy)_3](PF_6)_2$ molecule depicted in (c and f), will not be hindered by molecular damage created during device processing.

To verify that a continuous luminophore pad is printed using BA-LIFT and not a pinhole structure often characteristic of drop-on-demand techniques, we further examine the electrical performance of the device. Current density (J) versus applied voltage (V) (Fig. 4a) is seen to exhibit the expected trend of a proper light-emitting diode. The smooth nature of the curve and absence of spikes is indicative of a device that is free of short circuits. Likewise, the linearity of luminance (EL) versus current density (Fig. 4b) is also indicative of a properly functioning device. A luminance
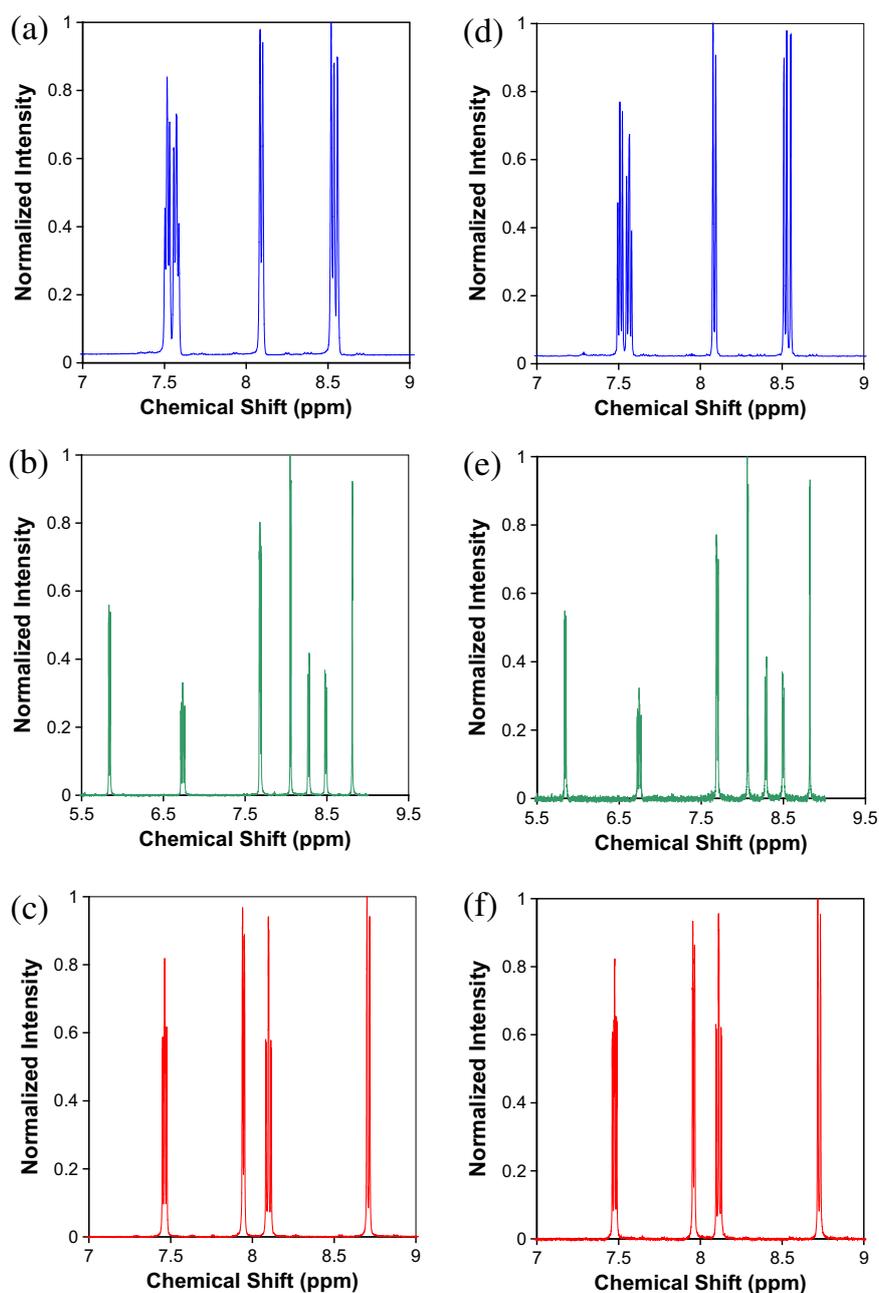

Fig. 3. Control sample NMR spectra for the (a) blue, (b) green, and (c) red molecule. BA-LIFT printed samples for the (d) blue, (e) green, and (f) red molecule display identical spectra to the control samples. The spectra from the blue molecule are reproduced from [11] for comparison. (For interpretation of the references to colour in this figure legend, the reader is referred to the web version of this article.)
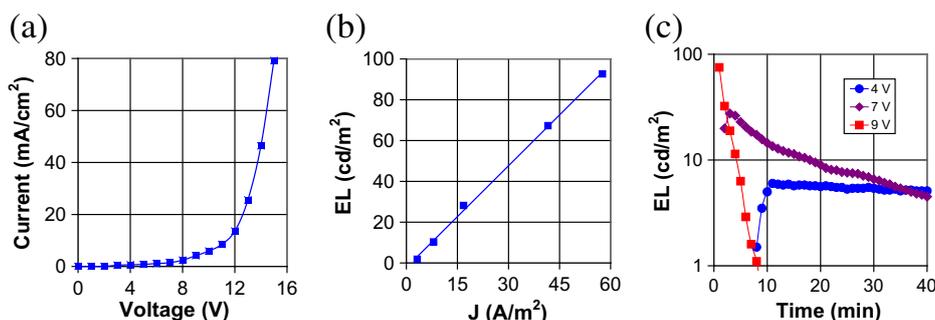
Fig. 4. (a) I–V and (b) EL-J measurements, and (c) time dependent EL of pristine devices for 3 bias voltages under ambient conditions.

of 93 cd/m^2 is measured at 11 V (Fig. 4b) with a device luminous efficiencies of roughly 0.39 ± 0.03 Lm/W at 3 V. This is comparable to literature values of 0.3 Lm/W given for devices fabricated by spin coating [Ru(bpy)$_3$]$^{2+}$(PF$_6^-$)$_2$, a molecule similar to ours, and vapor depositing a gold bottom electrode [25].

To probe the air stability of Complex **1** devices, time-dependent EL at different voltages is acquired from pristine, non-packaged and non-pre-biased devices (Fig. 4c). As expected, a reduction in turn on time and an increase in luminance is evident at higher voltages. However in accordance with literature observations, the benefits of higher voltage are outweighed by a reduction in device lifetime [5,22]. For example, at 9 V, (75 cd/m^2) peak luminance rapidly decays to its half life within two minutes of operation. The expected decrease in radiant flux is attributed to irreversible degradation of the molecule [20,22]. In contrast, a balance can be struck between peak luminance and device lifetime, through the application of a lower bias (7 V). Although device degradation rate is lower, it is still too high for practical purposes. A further decrease in applied voltage to 4 V can stabilize the device to a constant 6 cd/m^2 over 40 min. This measured lifetime increase is comparable to that reported in the literature [20] and is attributed to a combination of added poly(methyl methacrylate) and applied voltage close to the redox potential (2.5–3.0 V) [23]. We attribute the lower intensity relative to the literature to a thicker than optimal luminophore film. However, device intensity can be improved through

optimized luminophore concentration, better solvent selection, or through deliberate ligand modification [26].

While our results demonstrate the ability to print millimeter sized electroluminescent devices, higher-resolution patterning is desirable in many applications. In order to demonstrate the applicability of BA-LIFT as a technique capable of creating novel architectures, micron-sized arrays of ink voxels are printed from spin coated donor substrates. The ability to handle arbitrary inks is demonstrated by laser transferring an additional green fluorescing [Ir(F$_5$-mppy)$_2$(dtb-bpy)]$^+$(PF$_6^-$) (Complex **2**) molecule from a second donor substrate. Fig. 5a shows a phosphor array printed (fluence = 1.8 J/cm^2) from 7 μm polymer-film-coated donor substrates with an average voxel diameter of 80 μm. The irregularity in green versus red voxels is explained by a change in the overall solvent/solute surface tension which alters the voxels interaction with the receiver substrate and modifies the solute transport mechanism during solvent evaporation. More uniform voxels may be achieved by independently fine tuning each solvent for the particular molecule at hand, either through the selection of a different solvent or through the judicious combination of many. Nevertheless, the direct-write nature of BA-LIFT enables high-resolution luminophore patterning, through independent motion control of the receiver substrate, without the need for additional patterning steps. High throughput for large area coverage can be readily accomplished by high-speed laser scanning, splitting single beams into multiple beams, using patterned masks [27] or
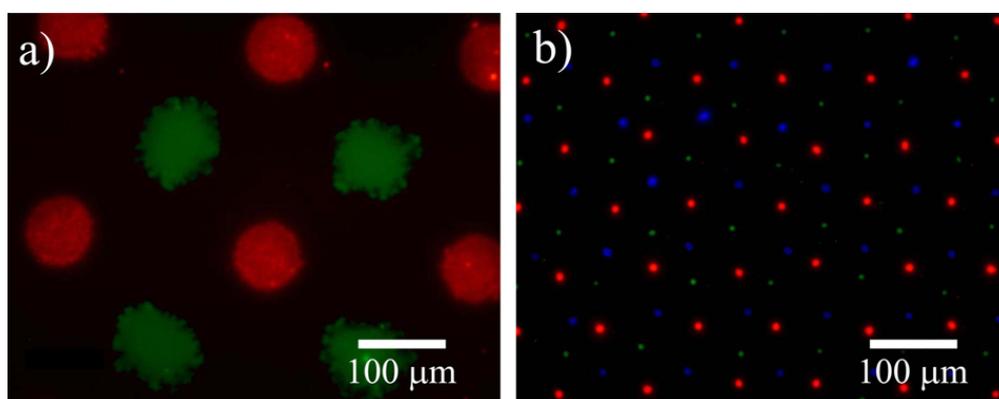

Fig. 5. (a) Fluorescent microscopy images of a typical luminophore array depicting voxel dimensions of approximately 80 μm. Ink/receiver surface tension sets the circumferential geometry. (b) Red, green, and blue voxel size is reduced to approximately 10 μm through BA-LIFT processing parameter optimization. (For interpretation of the references to colour in this figure legend, the reader is referred to the web version of this article.)

using arrays of glass microspheres [28,29] to generate high-resolution patterns.

Another attractive capability of BA-LIFT is the easy miniaturization of voxel size through processing parameter optimization. As a demonstration, a thinner polymer film thickness (4 μm) and lower fluence (0.7 J/cm^2) is selected based on previous knowledge that both quantities affect voxel size [18]. These processing parameters enable us to print multi-color voxel diameters of approximately 10 μm (Fig. 5b). Here an additional blue emitting 9-anthracenemethanol molecule (Complex **3**) is laser transferred to further demonstrate the technique's ability at printing the three colors found in standard organic light-emitting diode (OLED) display technologies. Transfers are conducted in a sequential manner from three luminophore-coated donor substrates to obtain multi-color printed arrays. Since all transfers are conducted at the same fluence, the small scatter in diameter size between colors is attributed to the variation in each of the inks fluid/substrate surface tension [30]. This can be easily controlled by altering the ink properties through small additions of different solvents to the host solution or by modulating the laser energy. Deviation in voxel diameter and position for a given color is primarily affected by statistical variations in the transferred droplet size due to the detailed fluid mechanics of the transfer process [18]. Size effects can be mitigated in a number of ways, for instance, by creating isolated wells in the donor substrate prior to transfer to pre-define the volume of transferred liquid [31], whereas positioning accuracy can be improved by reducing the spacing between the donor and receiving substrates. Nevertheless, resting voxel diameters of 10 μm are an appropriate size for future organic electronic technologies, and serve as a staring point to begin the study of structure–function relationships in these iTMCs.

4. Conclusion

This work presents a novel approach to printing light-emitting diodes from organo-metallic luminophore compounds. By employing air and moisture tolerant molecules, devices are fabricated in ambient conditions using a laser-based process termed BA-LIFT. The direct-write nature of this approach enables printing of the active organo-metallic luminophore with resolution down to 10 μm, without damage and without the need for masks, molds, etching, or vacuum processes. Devices are tested and shown to exhibit electroluminescence emission, diode behavior, and lifetimes in agreement with literature results for spin-coated devices fabricated in nitrogen environments. Our laser-based approach is compatible with rapid-prototyping and large-area electronics yet at the same time, the high printing resolution opens the door to novel experiments characterizing the structure–property relations for this important class of materials.

Acknowledgements

References

[1] S.E. Shaheen, D.S. Ginley, G.E. Jabbour, Organic-based photovoltaics: toward low-cost power generation, MRS Bull. 30 (2005) 10.

[2] F. So, J. Kido, P. Burrows, Organic light-emitting devices for solid-state lighting, MRS Bull. 33 (2008) 663.

[3] C.J. Brabec, J.R. Durrant, Solution-processed organic solar cells, MRS Bull. 33 (2008) 670.

[4] C.J. Brabec, J.A. Hauch, P. Schilinsky, C. Waldauf, Production aspects of organic photovoltaics and their impact on the commercialization of devices, MRS Bull. 30 (2005) 50.

[5] J.D. Slinker, J. Rivnay, J.A. Defranco, D.A. Bernards, A.A. Gorodetsky, S.T. Parker, M.P. Cox, R. Rohl, G.G. Malliaras, S. Flores-Torres, H.D. Abruña, Direct 120 V, 60 Hz operation of an organic light emitting device, J. Appl. Phys. 99 (2006) 074502.

[6] A.A. Gorodetsky, S. Parker, J.D. Slinker, D.A. Bernards, M.H. Wong, G.G. Malliaras, S. Flores-Torres, H.D. Abruña, Contact issues in electroluminescent devices from ruthenium complexes, Appl. Phys. Lett. 84 (2004) 807.

[7] J.D. Slinker, J. Rivnay, J.S. Moskowitz, J.B. Parker, S. Bernhard, H.D. Abruña, G.G. Malliaras, Electroluminescent devices from ionic transition metal complexes, J. Mater. Chem. 17 (2007) 2976.

[8] C.B. Arnold, P. Serra, A. Piqué, Laser direct-write techniques for printing of complex materials, MRS Bull. 32 (2007) 23.

[9] E. Menard, M.A. Meitl, Y. Sun, J.U. Park, D.J. Shir, Y.S. Nam, S. Jeon, J.A. Rogers, Micro- and nanopatterning techniques for organic electronic and optoelectronic systems, Chem. Rev. 107 (2007) 1117.

[10] S.H. Ko, H. Pan, S.G. Ryu, N. Misra, C.P. Grigoropoulos, H.K. Park, Nanomaterial enabled laser transfer for organic light emitting material direct writing, Appl. Phys. Lett. 93 (2008) 151110.

[11] N.T. Kattamis, N.D. McDaniel, S. Bernhard, C.B. Arnold, Laser direct write printing of sensitive and robust light emitting organic molecules, Appl. Phys. Lett. 94 (2009) 103306.

[12] L. Rapp, A.K. Diallo, A.P. Alloncle, C. Videlot-Ackermann, F. Fages, P. Delaporte, Pulsed-laser printing of organic thin-film transistors, Appl. Phys. Lett. 95 (2009) 171109.

[13] M. Kandyla, S. Chatzandroulis, I. Zergioti, Laser induced forward transfer of conducting polymers, Optoelectron. Rev. 18 (2010) 345.

[14] R. Fardel, M. Nagel, F. Nüesch, T. Lippert, A. Wokaun, Fabrication of organic light-emitting diode pixels by laser-assisted forward transfer, Appl. Phys. Lett. 91 (2007) 061103.

[15] R. Fardel, M. Nagel, F. Nüesch, T. Lippert, A. Wokaun, Laser-induced forward transfer of organic LED building blocks studied by time-resolved shadowgraphy, J. Phys. Chem. C 114 (2010) 5617.

[16] A.J. Birnbaum, H. Kim, N.A. Charipar, A. Pique, Laser printing of multi-layered polymer/metal heterostructures for electronic and MEMS devices, Appl. Phys. A 99 (2010) 711.

[17] M. Colina, M. Duocastella, J.M. Fernandez-Pradas, P. Serra, J.L. Morenza, Laser induced forward transfer of liquids: study of the droplet ejection process, J. Appl. Phys. 99 (2006) 84909.

[18] M.S. Brown, N.T. Kattamis, C.B. Arnold, Time-resolved study of polyimide absorption layers for blister-actuated laser-induced forward transfer, J. Appl. Phys. 107 (2010) 083103.

[19] N.T. Kattamis, P.E. Purnick, R. Weiss, C.B. Arnold, Thick film laser induced forward transfer for deposition of thermally and mechanically sensitive materials, Appl. Phys. Lett. 91 (2007) 171120.

[20] S. Bernhard, J.A. Barron, P.L. Houston, H.D. Abruña, J.L. Ruglovksy, X. Gao, G.G. Malliaras, Electroluminescence in ruthenium(II) complexes, J. Am. Chem. Soc. 124 (2002) 13624.

[21] J.D. Slinker, C.Y. Koh, G.G. Malliaras, M.S. Lowry, S. Bernhard, Green electroluminescence from an ionic iridium complex, Appl. Phys. Lett. 86 (2005) 173506.

[22] E.S. Handy, A.J. Pal, M.F. Rubner, Solid-state light-emitting devices based on the tris-chelated ruthenium(II) complex. 2. Tris(bipyridyl)ruthenium(II) as a high-brightness emitter, J. Am. Chem. Soc. 121 (1999) 3525.

[23] H. Rudmann, M.F. Rubner, Single layer light-emitting devices with high efficiency and long lifetime based on tris(2,2′bipyridyl) ruthenium(II) hexafluorophosphate, J. Appl. Phys. 90 (2001) 4338.

[24] V. Balzani, F. Barigelletti, L. Decola, Metal-complexes as light-absorption and light-emission sensitizers, Top. Curr. Chem. 158 (1990) 31.

[25] J.D. Slinker, A.A. Gorodetsky, M.S. Lowry, J. Wang, S. Parker, R. Rohl, S. Bernhard, G.G. Malliaras, Efficient yellow electroluminescence from a single layer of a cyclometalated iridium complex, J. Am. Chem. Soc. 126 (2004) 2763.

[26] R.D. Costa, E. Ortí, H.J. Bolink, S. Graber, C.E. Housecroft, M. Neuburger, S. Schaffner, E.C. Constable, Two are not always better than one: ligand optimisation for long-living light-emitting electrochemical cells, Chem. Commun. (2009) 2029.

[27] A. Narazaki, T. Sato, R. Kurosaki, Y. Kawaguchi, H. Niino, Nano- and microdot array formation of FeSi2 by nanosecond excimer laser-induced forward transfer, Appl. Phys. Express 1 (2008) 057001.

[28] C.M. Othon, A. Laracuente, H.D. Ladouceur, B.R. Ringeisen, Sub-micron parallel laser direct-write, Appl. Surf. Sci. 255 (2008) 3407.

[29] L. Landstrom, J. Klimstein, G. Schrems, K. Piglmayer, D. Bauerle, Single-step patterning and the fabrication of contact masks by laser-induced forward transfer, Appl. Phys. A-Mater. 78 (2004) 537.

[30] M.S. Brown, N.T. Kattamis, C.B. Arnold, Time-resolved dynamics of laser induced micro jets from thin liquid films, Microfluid. Nanofluid. (2011), doi:10.1007/s10404-011-0787-4.

[31] J.A. Barron, D.B. Krizman, B.R. Ringeisen, Laser printing of single cells: statistical analysis, cell viability, and stress, Anal. Biomed. Eng. 33 (2005) 121.